
Unifying Heterogenous Electronic Health Records Systems via Text-Based Code Embedding

Kyunghoon Hur^{1*}Jiyoung Lee^{1*}Jungwoo Oh¹Wesley Price²Young-Hak Kim³Edward Choi¹Graduate School of AI, KAIST, Daejeon, South Korea¹MIT, Cambridge, MA USA²

Department of Cardiology, Asan Medical Center,

University of Ulsan College of Medicine, Seoul, South Korea³

{pacesun, jiyounglee0523, ojw0123, edwardchoi}@kaist.ac.kr

wjprice@mit.edu

mdyhkim@amc.seoul.kr

Abstract

Substantial increase in the use of Electronic Health Records (EHRs) has opened new frontiers for predictive healthcare. However, while EHR systems are nearly ubiquitous, they lack a unified code system for representing medical concepts. Heterogeneous formats of EHR present a substantial barrier for the training and deployment of state-of-the-art deep learning models at scale. To overcome this problem, we introduce Description-based Embedding, DescEmb, a code-agnostic description-based representation learning framework for predictive modeling on EHR. DescEmb takes advantage of the flexibility of neural language understanding models while maintaining a neutral approach that can be combined with prior frameworks for task-specific representation learning or predictive modeling. We tested our model's capacity on various experiments including prediction tasks, transfer learning and pooled learning. DescEmb shows higher performance in overall experiments compared to code-based approach, opening the door to a text-based approach in predictive healthcare research that is not constrained by EHR structure nor special domain knowledge.

1 Introduction

Increased adoption of electronic health record (EHR) systems and growing computational power offer great potential for EHR-based predictive models to improve healthcare quality. In particular, deep learning models have shown comparable or better performance over domain experts in diagnosing or predicting various medical events, such as diseases or other patient outcomes [19, 13, 31]. These deep learning-based strategies rely on the accessibility of large and high-quality datasets in order to capture the complex semantics underlying EHR data.

However, inherent characteristics of EHR present unique barriers for real-world applications of EHR-based deep learning models. One primary difficulty stems from the heterogeneity of the code systems employed by the hospitals to represent clinical concepts in the data. Contemporary EHRs rely on data systems ranging from standardized codes (e.g. ICD9, LOINC) to hospital-specific systems

*Equal contribution

or free-text entry. Therefore, modern deep learning approaches for predictive healthcare are based on learning the representations of these codes, an approach we refer to as "code-based embedding." However, this paradigm does not allow flexible representation learning for medical concepts. In particular, code-based embedding limits the ability of prediction models to be transferred from one environment to another where different EHR formats are used. It also does not facilitate simple training of models on large EHR data collected from multiple hospitals that use heterogeneous EHR formats. Consequently, modern deep learning prediction models are missing out on the opportunity to be scaled up to multi-regional or even multi-national data. This challenge could be alleviated by mapping codes from one system to another, or by converting all EHR data to Common Data Model (e.g. OMOP, FHIR) [30]. However, even for a set of concepts as standardized as diagnosis codes, mapping codes from one system to another requires significant human effort and domain knowledge and may not even be possible, depending on the code system at hand.

In this paper, we address this challenge by suggesting a code-agnostic text-based representation learning in time-series patient data. Based on the idea that each medical code has a text description that represents its semantic property, we propose Description-based Embedding, DescEmb. DescEmb adopts a neural language understanding model (i.e. neural text encoder) to convert medical codes to contextualized embeddings, allowing us to map medical codes of different formats to the same text embedding space. Figure 1 gives a visual summary of our model framework; instead of directly embedding the medical codes as in (A), the prediction layer takes a series of vectors representing code descriptions passed through a neural text encoder as in (B) and (C). Our principled approach yields improved predictive performance compared to the Code-based Embedding, CodeEmb, and makes it possible to train models on differently formatted EHR data interchangeably due to its code-agnostic nature.

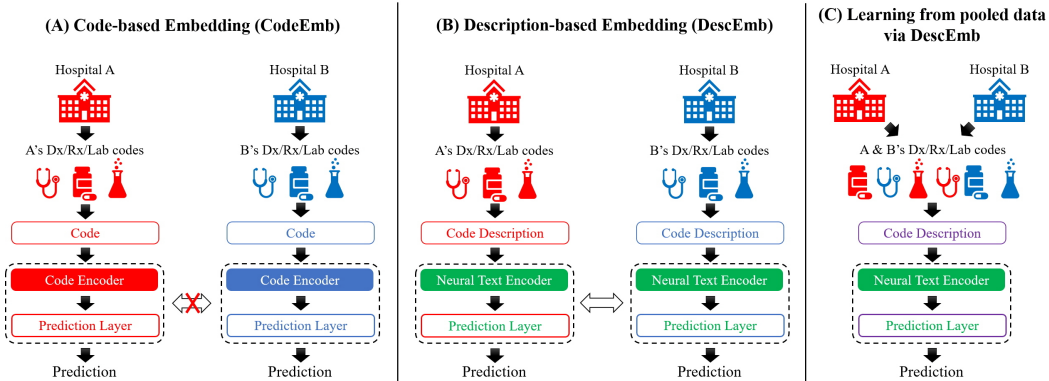


Figure 1: CodeEmb and DescEmb concept visualization. (A) CodeEmb: predictive models are trained with code-base embedding. The code encoders and the prediction layers cannot be shared among different hospitals due to heterogeneity of the code systems. (B) DescEmb: predictive models are trained on description-based embeddings derived from the text encoder. Due to the code-agnostic nature of the text-encoder, both the text encoders and the prediction layers can be transferred between different hospitals, unlike (A). (C) Learning from pooled data via DescEmb: we can pool heterogeneous hospital data into one dataset and train jointly, thus increasing the deployment efficiency.

We test our framework on two EHR datasets, the Medical Information Mart for Intensive Care (MIMIC-III) [14] and eICU Collaborative Research Database [29], which use completely different medical code systems. Based on extensive experiments using five prediction tasks under diverse settings (e.g. standard single-domain learning, zero-shot and few-shot transfer learning, pooled learning), the best model of DescEmb demonstrates superior or comparable performance to the best model of CodeEmb in the vast majority of cases, outperforming by an average of 2.6%P AUPRC.

The main contributions of our work can be summarized as follows:

1. DescEmb achieves comparable or superior performance to CodeEmb on a comprehensive set of common clinical predictive tasks. Detailed results can be found in Table 1, 2.

- Two differently structured EHR can be used to train and test predictive models interchangeably while rarely sacrificing model performance, often showing higher performance than when training on a single EHR. Visualized results can be found in Figure 4.
- Two differently structured EHR can be pooled into one dataset and trained jointly with a description-based representation without the need for additional preprocessing or domain knowledge. For the result, refer to Table 3.
- DescEmb shows notable performance in overall experiments, opening the door to a text-based approach in predictive healthcare research that is not constrained by EHR structure nor special domain knowledge.

2 Related Work

2.1 Neural Text Encoders

Contextualized word embeddings have become the backbone of many natural language processing (NLP) tasks. Early text embedders encode each word in a vocabulary as a vector whose semantic similarity to other words is represented by a distance measure (e.g. cosine similarity), or distribution of words [23, 27]. Recently, Bidirectional Encoder Representations from Transformers (BERT) and its variants [11, 15, 20, 38] have shown significant improvements on various tasks across NLP. Building on the Transformer architecture introduced by Vaswani et al. [37], BERT and similar models employ a unique pre-training strategy, Masked Language Modeling (MLM) and Next Sentence Prediction (NSP), to learn contextual text representations that enable the models to understand complex relationships within the input text.

Recent work has indicated that domain-specific pre-training can improve the performance of large language models like BERT, which rely on general domain text such as Wikipedia and BooksCorpus [41]. Particularly in the biomedical domain, several studies have developed BERT variants further trained on medical or clinical corpora in order to offer more precise contextualized embeddings for domain-specific tasks. Domain-specific BERT variants in the biomedical field have been continually pre-trained on research articles from PubMed [17], MIMIC-III clinical text [1], or a combination of the two [26], and scratch trained on articles from PubMed [12].

2.2 Representation Learning for Predictive Healthcare

A wide variety of deep learning models have been proposed over the past several years for predictive modeling with EHR data. Models based on autoencoders are used to learn patient representations for downstream prediction tasks [24, 2]. Given the sequential nature of the longitudinal EHR data, diverse works have been proposed to learn patient representations using recurrent neural networks (RNN) across objectives such as accurate prediction, interpretability, or scalability [19, 5, 4, 28, 21, 30, 36], while other works have focused predominantly on learning medical concept representations [6, 7, 22, 8, 35, 39, 40]. Other model architectures are also used for predictive healthcare such as gradient boosted machines [3], convolutional nets [25, 16], and Transformer-based models [34, 33, 9, 18, 32].

Throughout, previous research has sought to build more effective representations of patient data for predictive healthcare with minimal feature engineering. While all previous works make unique contributions to predictive healthcare in their own ways, their approach assumes that medical codes are the basic unit of processing, namely code-based embedding. Our paper focuses on a new problem setting—the unification of heterogeneous code systems in EHR—and therefore sits independent to these previous works. As such, our proposed approach can be readily combined with prior frameworks for any task-specific representation learning and predictive modeling.

3 Methods

3.1 Structure of Electronic Health Records

In this section, we describe the structure of EHR and introduce the notations to be used throughout the paper. Let p^i denote the i -th patient in the EHR data. As our problem setting is focused on individual patients, we drop the superscript when clear. A single patient p can be seen as a series of medical

events (c_1, c_2, \dots, c_T) for $c_i \in \mathcal{C}$ where \mathcal{C} denotes the set of all medical events such as diagnoses or prescriptions. Each event c_i is typically timestamped, giving us the sequence of time information (t_1, t_2, \dots, t_T) . Note that a series of medical events could be collected over a longer time period (e.g. outpatient records) or shorter time period (e.g. a single ICU stay).

A single medical event c_i is often associated with a text description. For example, if c_i were a prescription event, it could be accompanied by the medication name (e.g. ‘‘Aspirin 300mg Tab.’’). If it were a diagnosis event, it could come with an ICD-9 code (e.g. 401.9), which in turn has its own description (‘‘Unspecified essential hypertension’’). We use d_i to denote this text description, which consists of a sequence of words (or sub-words) $(w_{i,1}, w_{i,2} \dots, w_{i,n})$ for $w_{i,j} \in \mathcal{W}$ where \mathcal{W} is the entire vocabulary.

Typically, two different medical institutions employ different \mathcal{C} ’s, such as when one hospital uses ICD-9 diagnosis codes while another uses SNOMED diagnosis codes. The vocabulary \mathcal{W} , however, is the same for all hospitals as long as they use the same language. We propose DescEmb, a new framework for predictive healthcare, based on this observation.

3.2 Model Architecture

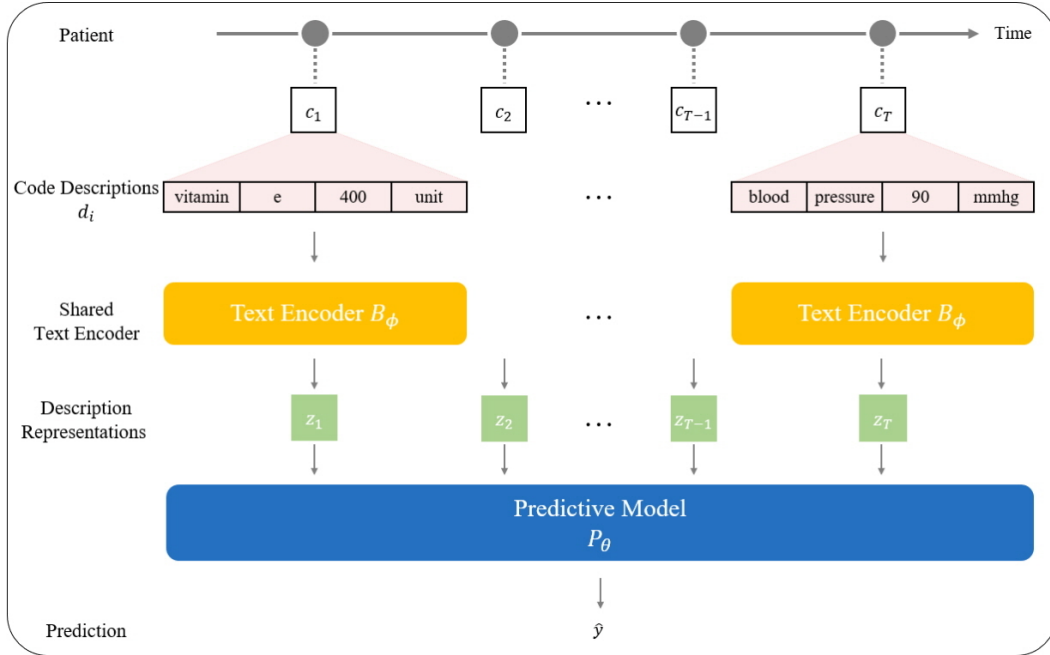


Figure 2: DescEmb model framework. On the top, the patient timeline from the ICU admission is represented as a line. Each dot on the line is a code c_i which can be any medical event. Each code c_i can be converted to its own description d_i . The neural text encoder B_ϕ accepts the description d_i and produces its latent representation z_i . Given all z_1, z_2, \dots, z_T , the predictive model P_θ predicts the outcome \hat{y}

Previous deep learning predictive models for EHR data typically have an embedding layer (or a lookup table) E_ψ with trainable parameters ψ , which converts a single medical event c_i to its corresponding vector representation $\mathbf{c}_i \in \mathbb{R}^a$ where a is the dimension size. Due to this architecture, a model trained on one hospital’s records would be expected to suffer significant performance decrease when deployed to another hospital with a completely different \mathcal{C} (Fig. 1 (A)). Instead of directly converting c_1, \dots, c_T to $\mathbf{c}_1, \dots, \mathbf{c}_T$ with a trainable lookup table, DescEmb derives the latent representation of c_i , denoted as \mathbf{z}_i , based on its text description d_i . We feed d_i to the shared text encoder, B_ϕ , to obtain the description representations, $\mathbf{z}_i \in \mathbb{R}^b$ where b is the output dimension. Repeating this for all events in the given patient p , we can obtain a sequence of contextualized medical event representations $(\mathbf{z}_1, \mathbf{z}_2, \dots, \mathbf{z}_T)$, which in turn is given to the prediction layer P_θ (e.g. RNN) with trainable parameters θ to make a prediction \hat{y} (Fig 2.) The entire process of DescEmb can be summarized as below, with

comparison to CodeEmb.

Given a patient record $p = (c_1, c_2, \dots, c_T)$,

Code-based Embedding:

$$\begin{aligned} \mathbf{c}_i &= E_\psi(c_i) \\ \hat{y} &= P_\theta(\mathbf{c}_1, \mathbf{c}_2, \dots, \mathbf{c}_T) \end{aligned} \tag{1}$$

Description-based Embedding:

$$\begin{aligned} d_i &= (w_{i,1}, w_{i,2}, \dots, w_{i,n}) \\ \mathbf{z}_i &= B_\phi(d_i) \\ \hat{y} &= P_\theta(\mathbf{z}_1, \mathbf{z}_2, \dots, \mathbf{z}_T) \end{aligned} \tag{2}$$

3.3 Text Encoder

The text encoder B_ϕ in DescEmb can be any type of model capable of generating the representation \mathbf{z}_i from a given description d_i . In this paper, we tested two main model architectures for the text encoder: Bi-Directional Recurrent Neural Networks (Bi-RNN) and Bidirectional Encoder Representations from Transformers (BERT). For Bi-RNN, we derived the \mathbf{z}_i by concatenating the last hidden states from each direction. For BERT, we used the output vector from the [CLS] token as \mathbf{z}_i . We conducted experiments on different sizes of models that are already pre-trained on a massive amount of general text such as Bert-tiny (2-layers), Bert-mini (4-layers), Bert-small (4-layers), Bert-base (12-layers).

We additionally conducted experiments on BERTs that are pre-trained intensively on clinical text, such as BioBERT [17], ClinicalBERT [1], and BlueBERT [26]. In order to assess the effectiveness of domain-specific pre-training, we compared these models with BERTs that are pre-trained on the general domain. (results can be found in Appendix A). Moreover, we further pre-trained the text encoder on our dataset using Masked Language Modeling (MLM), following the original BERT procedure, to better fit the text encoder to our dataset. We did not include values during MLM since predicting values from descriptions is meaningless considering the various patient statuses.

3.4 Value Embedding

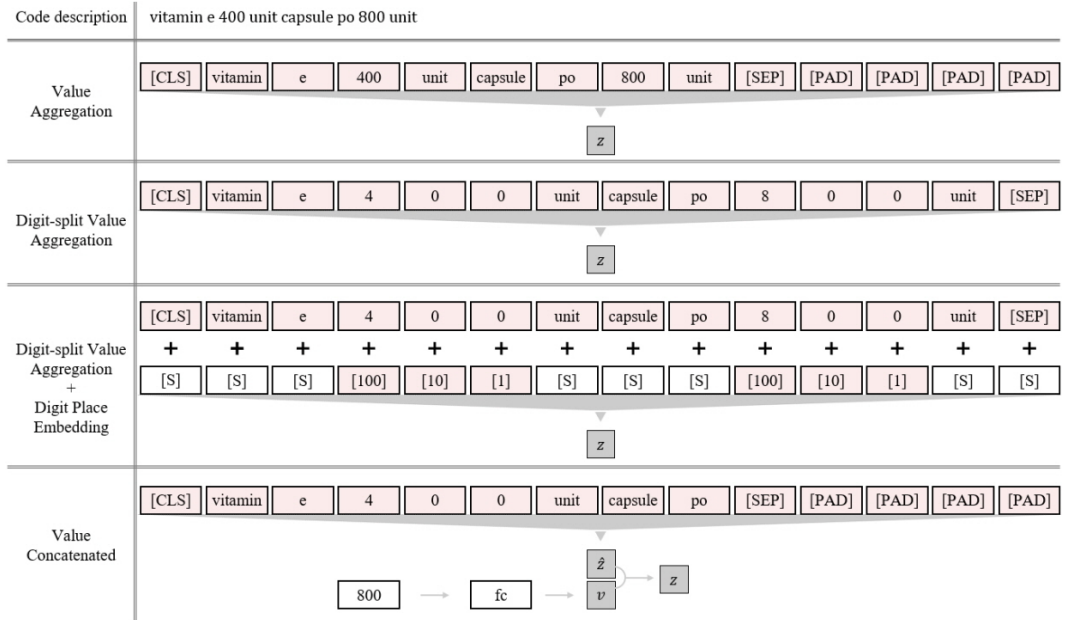


Figure 3: Various methods of incorporating numeric values. In order to effectively represent both the code descriptions and the associated numeric values (e.g. “10” in “Tylenol 10 tabs”), we introduce four different value embedding methods.

In the context of drug prescriptions, dosage or rate of infusion can be useful information to represent the patient’s status. Also, laboratory measures, such as blood pressure or glucose level measure, can also be a good indicator of the patient status. Hence, values incorporated in a code description provide rich informative features to the model, potentially leading to an increase in the prediction performance. When using DescEmb, both the code description d_i and the associated numeric values can be embedded with the text encoder B_ϕ .

As shown in Figure 3, we introduce four different value embedding methods. First, Value Aggregation (VA) stands for aggregating the code description and the numeric values together as text. In this setting, because the BERT tokenizer recognizes each value as a word, it sometimes tokenizes a given value in an unnatural way. For example, a number ‘1351’ can be split into two sub-words ‘13’ and ‘51’, which does not best reflect the underlying meaning of the number. Hence, we additionally propose Digit-Split Value Aggregation (DSVA), where we split all numeric values into each digit first, then aggregate with the code description as text. In this way, a number is always tokenized into single digits, but the model still does not consider the place value. For instance, a number ‘1351’ will be tokenized into ‘1’, ‘3’, ‘5’, ‘1’; the model recognizes the first ‘1’ and the last ‘1’ as the same token even though the first ‘1’ represents the thousandth place and the last ‘1’ represents the first place. To mitigate this misunderstanding, we add learnable Digit Place Embedding (DPE) to every digit token indicating its place value, named Digit-Split Value Aggregation + Digit Place Embedding (DSVA+DPE). This can only be applied to the model exploiting a neural text encoder which can add additional value embedding for each digit. Value Concatenated (VC) embeds description and values separately. Similar to the other embedding methods, code description and unit of measurement are embedded through the text encoder, while values are passed through additional Multi-Layer Perceptron (MLP) which yields an embedding vector for the values. These two embeddings are finally concatenated and work as a description representation z_i for input of the predictive model.

3.5 Model Optimization

Both CodeEmb and DescEmb are used for prediction, therefore we can use any typical prediction loss function \mathcal{L} such as the cross-entropy loss or mean squared error. For DescEmb, training an entire BERT-like text encoder B_ϕ while optimizing predictive model P_θ requires a significant amount of time and compute resources, which are often inaccessible by small hospitals. Therefore, we propose the following light-weight DescEmb method, CLS-finetune. The objective functions of each model are shown below.

$$\textit{Code-based Embedding} \qquad \underset{\theta, \psi}{\operatorname{argmin}} \mathcal{L}(y, \hat{y}) \qquad (3)$$

$$\textit{Description-based Embedding} \qquad \underset{\theta, \phi}{\operatorname{argmin}} \mathcal{L}(y, \hat{y}) \qquad (4)$$

$$\textit{Description-based Embedding CLS-finetune} \qquad \underset{\theta, z_{CLS}}{\operatorname{argmin}} \mathcal{L}(y, \hat{y}) \qquad (5)$$

CLS-finetune, as written in Eq. 5, keeps ϕ of the text encoder fixed but allows for fine-tuning only the medical event embeddings z_{CLS} derived from B . This can also be seen as initializing the parameters of the embedding layer E_ψ with the values of z_{CLS} , instead of initializing with random values. CLS-finetune does not solely rely on B ’s ability to derive medical event embeddings, but allows flexibility for the model to adapt to given prediction task with reasonable computation overhead.

4 Experiments

4.1 Datasets

We draw on two large, publicly available datasets to demonstrate our model concept: the Medical Information Mart for Intensive Care III (MIMIC-III) [14], and the eICU Collaborative Research Database (eICU) [29]. MIMIC-III includes all patients admitted to the intensive care unit (ICU) at Beth Israel Deaconess Medical Center from 2001 to 2012, and contains over 60,000 unique ICU stays with millions of observations. The eICU Collaborative Research Database is a multi-center database comprised of de-identified health data associated with over 200,000 ICU stays across the United States between 2014-2015.

Both MIMIC-III and eICU contain time-stamped records of medical events such as labs, medications, and drug inputs for each patient stay. Important for our proposed framework, MIMIC-III and eICU are recorded based on completely different code structures throughout the data. For example, the clinical concept “an infusion event of nitroglycerin” is represented in eICU as the string “Nitroglycerin (mcg/min)”. However, the same semantic concept would be represented in MIMIC-III using the in-house item ID 222056 (a Metavision code, for "Nitroglycerin"); item ID 30049 (a CareVue code, for "Nitroglycerin"); or item ID 30121 (a CareVue code, for "Nitroglycerin-k"). The same goes for all medical events including diagnosis, medications, labs, etc. Consequently, we aggregate descriptions and values for comparability between formats and do not perform any within-code string manipulation. Detailed data preprocessing is provided in Appendix C.

4.2 Prediction Tasks

We examine a total of five prediction tasks based on individual ICU stays to assess the feasibility of our model: readmission, mortality, length of stay (exceeding 3 days and 7 days), and diagnosis prediction. Note that a patient can have more than one ICU stay during their entire hospital stay; however, we only use the first stay of our predictions. Each task is defined as follows:

Readmission Prediction (Binary Prediction): Given a single ICU stay, we consider this sample readmitted if it is followed by another ICU stay during the same hospital stay

Mortality Prediction (Binary Prediction): A sample is labeled positive for mortality if the discharge state was “expired”.

Length-of-Stay Prediction (Binary Prediction): There are two cases for length of stay (LOS) prediction; whether a given ICU stay lasted longer than 3 days, and whether it lasted longer than 7 days.

Diagnosis Prediction (Multi-Label Prediction): Given all diagnosis codes accumulated during the entire hospital stay, we group them into 18 diagnosis classes of the Clinical Classification Software (CCS) for ICD-9-CM criteria [10]. The target label for a given ICU stay is generated as CCS classes in one-hot vector form. The detailed process for generating labels is discussed in Appendix C.2.

4.3 Implementation Details

We select a subset of patient records from MIMIC-III and eICU in order to perform clinically meaningful predictions with matched cohort characteristics. In particular, we select the first 12 hours of the first ICU stay of medical ICU (MICU) patients over the age of 18. We draw on a combination of laboratory measurements, medications prescribed, and infusion events aligned into a sequence by time stamps. These steps produce 12,818 samples from eICU and 18,536 samples from MIMIC-III. We randomly split the data into training, validation, and test sets according to a 65:15:20 ratio. Further details regarding data preprocessing are described in Appendix C.1.

All models were implemented with PyTorch. For BERT-based text encoders, we use the pre-trained models available in the HuggingFace GitHub repository to initialize the weights of B_ϕ . For the prediction model P_θ , we used an RNN, a widely used prediction model for healthcare prediction. Each experiment was evaluated using 10 random seeds, using area under precision recall curve (AUPRC) for binary classification tasks (readmission, mortality, LOS>3days, LOS>7days) and micro-averaged AUPRC (micro-AUPRC) for diagnosis classification. Evaluation metrics are reported throughout the paper as the mean of the ten seed experiments. We employ one fixed set of hyperparameters for all experiments; specific values are reported in Appendix C.4.

4.4 Prediction Performance

To assess the general efficacy of the DescEmb framework, we evaluate both DescEmbs and CodeEmbs across five medical prediction tasks using two separate datasets. The results are in Table 1 and Table 2. Value embedding methods are abbreviated as explained in the method section. The results for DSVA + DPE in CodeEmb and CLS-FT are blank since they cannot use Digit Place Embedding. In CodeEmb, ‘RD’ represents a randomly initialized embedding layer while ‘W2V’ represents Word2Vec, a pre-training strategy for CodeEmb embedding layer [23]. ‘FT’ stands for fine-tuning where we employ existing pre-trained BERT parameters and fine-tune them for the downstream tasks. ‘Scr’ stands for

training from scratch where we do not bring the pre-trained BERT but randomly initialize the model. ‘FT + MLM’ is a model that brings a pre-trained model and conducts Masked Language Modeling (MLM) on our dataset after which it is fine-tuned on downstream tasks. ‘Scr + MLM’ is similar to ‘FT + MLM’ but it does not bring the pre-trained model parameter. We utilize the BERT-Tiny architecture for the BERT-based text encoder because there was no significant performance difference among BERT variants across sizes and pre-training techniques specific to clinical domain corpus; detailed results on this part can be found in Appendix A.

Table 1: AUPRC of CodeEmbs and DescEmbs in prediction tasks for eICU

Task	Model	CodeEmb		DescEmb					
				BERT				RNN	
				RD	W2V	CLS-FT	FT	Scr	FT + MLM
Dx	VA	0.447	0.433	0.501	0.574	0.547	0.586	0.586	0.582
	DSVA	0.447	0.433	0.498	0.591	0.567	0.601	0.593	0.584
	DSVA+DPE	-	-	-	0.594	0.571	0.602	0.594	0.583
	VC	0.562	0.549	0.557	0.562	0.546	0.555	0.557	0.557
Mort	VA	0.112	0.153	0.209	0.177	0.17	0.216	0.237†	0.271
	DSVA	0.112	0.153	0.209	0.223	0.215	0.213	0.235	0.247
	DSVA+DPE	-	-	-	0.224	0.213	0.217	0.252	0.259
	VC	0.24†	0.239†	0.238†	0.23†	0.23†	0.223	0.237†	0.227†
LOS>3	VA	0.47†	0.439	0.533	0.52	0.511	0.514	0.537	0.539
	DSVA	0.47†	0.439	0.529	0.53	0.538	0.529	0.539	0.537
	DSVA+DPE	-	-	-	0.536	0.537	0.529	0.54	0.537
	VC	0.525	0.525	0.528	0.523	0.524	0.523	0.526	0.53
LOS>7	VA	0.157	0.184	0.225	0.196†	0.185	0.196	0.224	0.237
	DSVA	0.157	0.184	0.225	0.216	0.222	0.221	0.227	0.233
	DSVA+DPE	-	-	-	0.22	0.219	0.221	0.231	0.234
	VC	0.231	0.228	0.229	0.216	0.218	0.218	0.222	0.224
ReAdm	VA	0.168	0.15	0.208	0.283	0.205	0.283	0.269	0.279
	DSVA	0.168	0.15	0.206	0.284	0.264	0.29	0.28	0.275
	DSVA+DPE	-	-	-	0.289†	0.263	0.284	0.28	0.255
	VC	0.217†	0.183†	0.194	0.272	0.256	0.267	0.277	0.276

†: standard deviation > 0.02

DescEmb models achieve comparable or superior performance to CodeEmb on nearly every task across all value embedding methods at the average of 8%P with 12%P at maximum. Within DescEmb models, BERT-FT generally outperforms BERT-Scratch, verifying the effectiveness of pre-training on massive text corpus. Using the additional Masked Language Modeling (MLM) on our dataset marginally improved performance (+0.3%P AUPRC) for BERT models. We further test the efficacy of MLM in the transfer learning setting below. Of note, a Bi-RNN text encoder generally performs better than BERT-based models. We speculate that, since the maximum lengths of sub-tokens for one code description are 46 and 48 for MIMIC-III and eICU respectively, a simple and light-weighted text encoder model, in this case Bi-RNN, has enough capacity to grasp the features of descriptions. In other words, a large and complex model, in this case BERT, might be an excessively powerful tool to compute refined representations in our setting.

Note that CLS-finetune in DescEmb, which requires the same amount of compute and time as CodeEmb but initializes the embeddings with the CLS outputs from pre-trained BERT, outperforms CodeEmb in nearly all cases. This demonstrates that there is ground to be gained by adopting description-based embedding compared to the classical code-based embedding. We also pre-train the CodeEmb’s embedding layer in Word2Vec manner to have a fair comparison with the pre-trained DescEmb models. We observe that Word2Vec results are highly unstable, which sometimes underperform 3.4%P at the worst compared to randomly initialized CodeEmb. This result implies that pre-training at code-level is insufficient to fully capture the semantics of each code and sometimes

Table 2: AUPRC of CodeEmb and DescEmb in prediction tasks for MIMIC-III.

Task	Value Embedding	CodeEmb		DescEmb					
		RD	W2V	BERT			RNN		
				CLS-FT	FT	Scr	FT + MLM	Scr	Scr + MLM
Dx	VA	0.726	0.704	0.733	0.76	0.747	0.767	0.767	0.762
	DSVA	0.726	0.704	0.731	0.77	0.752	0.776	0.77	0.766
	DSVA+DPE	-	-	-	0.771	0.752	0.764	0.768	0.763
	VC	0.757	0.751	0.752	0.756	0.745	0.75	0.755	0.753
Mort	VA	0.228	0.209	0.346	0.343†	0.31	0.38	0.383	0.398
	DSVA	0.228	0.209	0.347	0.377	0.378	0.379	0.394†	0.39
	DSVA+DPE	-	-	-	0.378	0.372	0.383	0.4	0.393
	VC	0.313†	0.334	0.339	0.336†	0.335†	0.376	0.344†	0.338
LOS>3	VA	0.582	0.585	0.608	0.616	0.601	0.616	0.624	0.63
	DSVA	0.582	0.585	0.608	0.624	0.617	0.619	0.631	0.632
	DSVA +DPE	-	-	-	0.624	0.616	0.622	0.634	0.628
	VC	0.61	0.614	0.616	0.61	0.614	0.612	0.622	0.622
LOS>7	VA	0.269	0.251	0.346	0.338	0.325	0.342	0.349	0.349
	DSVA	0.269	0.251	0.348	0.355	0.359	0.356	0.35	0.35
	DSVA+DPE	-	-	-	0.36	0.359	0.353	0.352	0.353
	VC	0.326	0.342	0.346	0.341	0.339	0.344	0.347	0.352
ReAdm	VA	0.044	0.043	0.042	0.042	0.045†	0.044	0.044	0.043
	DSVA	0.044	0.043	0.041	0.043	0.046†	0.044	0.045	0.044
	DSVA+DPE	-	-	-	0.043	0.047	0.044	0.041	0.044
	VC	0.043	0.043	0.044	0.045	0.047	0.044	0.044	0.044

†: standard deviation > 0.02

harms the performance. On the other hand, all pre-trained DescEmb models consistently show high performance across all scenarios verifying the robustness of pre-training at description-level.

For value embeddings, there is a large discrepancy between CodeEmbs and DescEmbs in Value Aggregation (VA) and Digit-Split Value Aggregation (DSVA) compared to other value embedding methods. We conjecture the underlying reason is that in VA and DSVA, the unique number of codes for CodeEmb explodes since a new code is needed when different values are used. This raises the curse of dimensionality. On the contrary, the unique number of sub-tokens used in DescEmb does not change significantly in either setting, resulting in a stable performance. Hence, DescEmb is a suitable model architecture for understanding values because it does not require creating a new code for different values. Value Concatenated (VC) performs the best in CodeEmb. In DescEmb, Digit-Split Value Aggregation with Digit Place Embedding (DSVA+DPE) shows higher performance on the whole than other value embedding methods. It explains that the model has better numeric understanding since DPE explicitly notifies the model about the place value. For further experiments, we choose CodeEmb RD, FT-BERT, SC-RNN, SC-RNN + MLM, with VC for CodeEmb and DSVA+DPE for the DescEmb models.

4.5 Zero-Shot Transfer and Few-Shot Transfer

Because DescEmb’s embedding space is determined not by a specific code structure, but rather by the language of the underlying text descriptions, our framework lends itself naturally to transfer learning across all hospitals regardless of their EHR format. On the other hand, in order to deploy a code-based model on a target dataset with a different code structure than the source dataset, the new code embeddings received by the predictive layer must be randomly initialized, as E_ψ is not shared between hospitals. Consequently, CodeEmb’s zero-shot transfer can rely only on the predictive layer parameters whereas DescEmb allows additional flexibility by relying on the B_ϕ parameters. Here, we transfer one CodeEmb model and three DescEmb models: RD, FT-BERT, SC-RNN, and

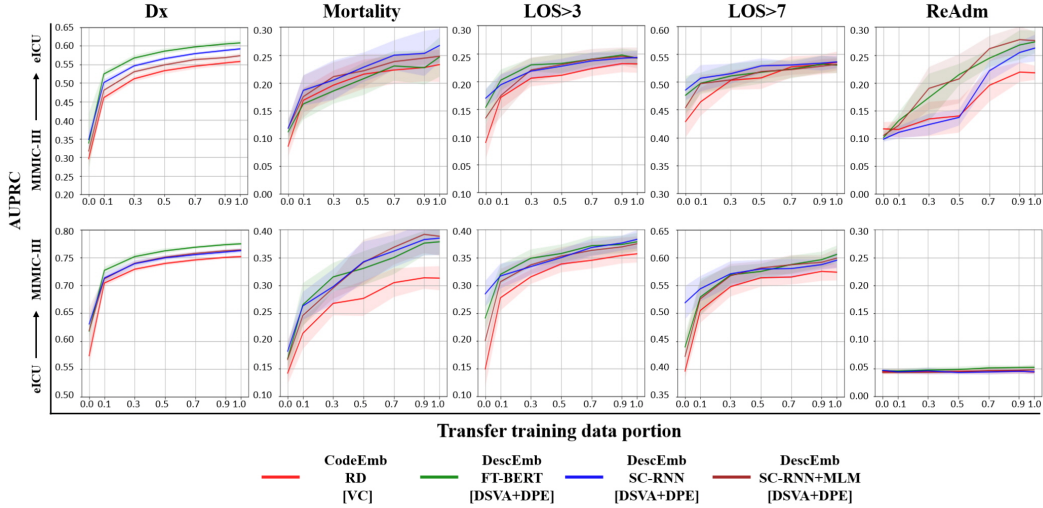


Figure 4: Transfer learning performance (Top: MIMIC-III to eICU, Bottom: eICU to MIMIC-III). The X-axis is the portion of the target dataset used for transfer learning, and the Y-axis is the AUPRC at test time on the target dataset. Shades represent the standard deviation from ten seed experiments.

SC-RNN+MLM trained on the MIMIC-III to eICU dataset and vice versa on zero shot and multiple few shot ratios. For SC-RNN+MLM, we did not conduct additional MLM on the target dataset before the transfer. The results are shown in Figure 4.

We observe predominantly higher performance of DescEmb over CodeEmb in both the zero-shot and few-shot transfer setting. When this is the case (that is, for all tasks except readmission prediction), DescEmb gains a particular advantage in zero-shot and smaller few-shot ratio transfer learnings, especially for the length-of-stay prediction tasks. This implies that DescEmb can be transferred to different hospitals while retaining its performance even for hospitals with a very small amount of data. We may intuitively understand these results as the uphill battle faced by the CodeEmb to adjust to a completely unfamiliar set of code embeddings—a disadvantage alleviated by a text-based framework and consequently not shared by DescEmb’s predictive layer. Even with a very limited amount of (or no) fine-tuning data from the target dataset, DescEmb can use its knowledge of a prior dataset’s text descriptions to generate effective embeddings at the outset.

4.6 Pooled Learning with Distinct EHR Formats

If we were to deploy a large-scale predictive model in reality, it is more likely that a single central server would pool EHR data from multiple institutions and train a large-scale deep learning model, rather than training many models from individual institutions and performing transfer learning when necessary. Such *pooled learning* presents an opportunity to train a single model to jointly learn information from all institutions. Applying CodeEmb to pooled learning, however, requires either substantial effort to unify code systems (if possible) or relinquishing control over the code vocabulary. Therefore, there is limited benefit of pooled learning for CodeEmb since it consumes a substantial amount of time and labor. Conversely, given that DescEmb is not restricted by specific code structures, pooling datasets does not require any further preprocessing nor extra investment of time and money.

In order to confirm the efficacy of DescEmb in the pooled learning scenario, we trained both DescEmb and CodeEmb on the pooled training set from both MIMIC-III and eICU, and tested on the individual test set. The results are reported in Table 3 where we compare model performance across various scenarios: train then evaluate on each dataset (“Single MIMIC-III” and “Single eICU”), train on one dataset then fine-tune and evaluate on another dataset (“Transfer eICU→MIMIC-III” and “Transfer MIMIC-III→eICU”), and train on the pooled dataset then evaluate on each dataset (“Pooled MIMIC-III” and “Pooled eICU”). We include both “Single” and “Transfer”, both of which require individual

Table 3: Single domain learning vs transfer learning vs pooled learning. Single domain results are drawn from Table 1 and Table 2, where a model was trained on one dataset. “Transfer” results are the same as the point at X-axis 1.0 in Figure 4 (i.e. transfer learning on the entire target dataset). “Pooled” learning is training models on the merged training sets of MIMIC-III and eICU, after which the model is tested on each test dataset. Based on t-test, statistically meaningful increase and decrease against “Single” is marked with boldface and underline, respectively.

Task	Model	Single MIMIC-III	Transfer eICU → MIMIC-III	Pooled MIMIC-III	Single eICU	Transfer MIMIC-III → eICU	Pooled eICU
Dx	CodeEmb	0.757	<u>0.752**</u>	0.755	0.562	0.558	0.563
	FT-BERT	0.771	0.775*	0.777*	0.594	0.608**	0.611*
	SC-RNN	0.768	0.762	0.773**	0.594	0.602**	0.589
	SC-RNN+MLM	0.763	0.76	0.768	0.583	0.586	0.595*
Mort	CodeEmb	0.313	0.313	0.313	0.24	0.233	0.247
	FT-BERT	0.378	0.378	0.376	0.224	0.246*	0.248*
	SC-RNN	0.4	0.385	0.401	0.252	0.267*	0.252
	SC-RNN+MLM	0.393	0.383	0.402	0.259	0.263	0.253
LOS>3	CodeEmb	0.61	0.606	0.611	0.525	0.531	0.534*
	FT-BERT	0.624	0.628*	0.624	0.536	0.542*	0.549*
	SC-RNN	0.634	0.632	0.63	0.54	0.543	0.549*
	SC-RNN+MLM	0.628	0.627	0.638*	0.537	0.541	0.548*
LOS>7	CodeEmb	0.326	0.333	0.334	0.233	0.235	0.239*
	FT-BERT	0.36	0.356	0.354	0.22	0.230*	0.242**
	SC-RNN	0.352	0.345	0.35	0.229	0.236*	0.253**
	SC-RNN+MLM	0.353	0.342	0.342	0.234	0.235	0.239*
ReAdm	CodeEmb	0.043	0.044	0.049	0.217	0.218	0.232*
	FT-BERT	0.043	0.044	0.051	0.289	<u>0.274*</u>	0.281
	SC-RNN	0.041	0.045	0.046	0.28	0.263	0.279
	SC-RNN+MLM	0.044	0.044	0.044	0.255	0.255	0.275*

* : p value < 0.05

** : p value < 0.01

model training on each dataset, to highlight the operational efficiency of pooled learning, which only requires a single model training on the pooled dataset.

Within pooled learning, DescEmb outperformed CodeEmb in all cases (8.9%P at most) except for readmission prediction for MIMIC-III, which indicates that DescEmb is clearly a more suitable framework for pooled learning. Of note, DescEmb’s pooled training showed favorable results compared to the single domain setting as well as transfer learning setting for both MIMIC-III and eICU (more so for eICU which we analyze below). This indicates the efficiency of pooled learning with DescEmb, where only a single model needs to be trained and maintained, instead of training or transferring individual models for each dataset. Thanks to this efficiency, we believe DescEmb can open new doors for large-scale predictive models in terms of operational cost in finance and time.

4.7 Representation Distribution and Pooled Learning Advantages

From Table 3, we can see that eICU generally gained more performance increase than MIMIC-III from both pooled learning and transfer learning. We hypothesize that this comes from the data distribution properties of the two datasets. In order to confirm our hypothesis, we conducted Principal Component Analysis (PCA) on the ICU stay representation vectors obtained from the prediction model (the last hidden layer of the RNN) trained on the pooled dataset. The results in Figure 5 show that, for some tasks, the eICU representations are distributed inside the MIMIC-III representation distributions, especially in LOS tasks where eICU gained notable performance increase from transfer

and pooled learning compared to the single-domain learning. We deduce that the performance increase comes from learning a more generally distributed dataset, in this case MIMIC-III.

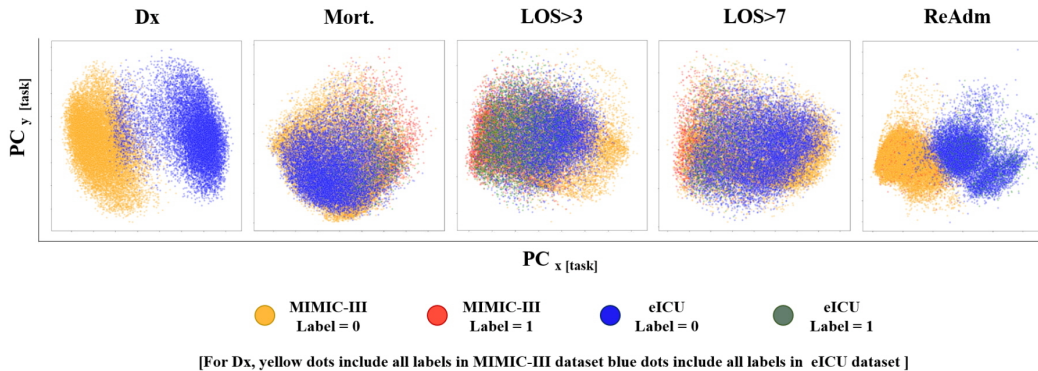


Figure 5: PCA visualizations of the ICU representations from the two datasets. The X-axis and Y-axis correspond to two different principal components. Each dot represents one ICU stay, and the dot color represents the target label for binary classification tasks. For the diagnosis prediction task (Dx), labels could not be succinctly annotated due to its multi-label classification nature. Thus, we distinguish dataset sources by color: yellow being MIMIC-III and blue being eICU.

5 Conclusion

In this work we introduced a new predictive modeling framework for EHR, namely the description-based embedding (DescEmb), which unifies heterogeneous code systems by deriving the medical code embeddings with a neural text encoder. In a series of experiments with two public EHR datasets and five ICU-based prediction tasks, we demonstrated DescEmb’s outperformance against CodeEmb. We also showed improved zero-shot and few-shot transfer learning performance thanks to the code-agnostic nature of DescEmb. Lastly, we showed that DescEmb provides operational efficiency by enabling us to train a single unified predictive model based on multiple heterogeneous EHR datasets, rather than training separate models for each EHR system. We believe this new framework will launch new discussion around large-scale model training for EHR, and we aim to incorporate additional modalities such as clinical notes or radiology images in future work.

References

- [1] Emily Alsentzer, John Murphy, William Boag, Wei-Hung Weng, Di Jindi, Tristan Naumann, and Matthew McDermott. 2019. Publicly Available Clinical BERT Embeddings. In *Proceedings of the 2nd Clinical Natural Language Processing Workshop*. Association for Computational Linguistics, Minneapolis, Minnesota, USA, 72–78. <https://doi.org/10.18653/v1/W19-1909>
- [2] Zhengping Che, David Kale, Wenzhe Li, Mohammad Taha Bahadori, and Yan Liu. 2015. Deep computational phenotyping. In *Proceedings of the 21th ACM SIGKDD International Conference on Knowledge Discovery and Data Mining*. 507–516.
- [3] David Chen, Sijia Liu, Paul Kingsbury, Sunghwan Sohn, Curtis B Storlie, Elizabeth B Habermann, James M Naessens, David W Larson, and Hongfang Liu. 2019. Deep learning and alternative learning strategies for retrospective real-world clinical data. *NPJ digital medicine* 2, 1 (2019), 1–5.
- [4] Edward Choi, Mohammad Taha Bahadori, Joshua A Kulas, Andy Schuetz, Walter F Stewart, and Jimeng Sun. 2016. Retain: An interpretable predictive model for healthcare using reverse time attention mechanism. *arXiv preprint arXiv:1608.05745* (2016).
- [5] Edward Choi, Mohammad Taha Bahadori, Andy Schuetz, Walter F Stewart, and Jimeng Sun. 2016. Doctor ai: Predicting clinical events via recurrent neural networks. In *Machine learning for healthcare conference*. PMLR, 301–318.
- [6] Edward Choi, Mohammad Taha Bahadori, Elizabeth Searles, Catherine Coffey, Michael Thompson, James Bost, Javier Tejedor-Sojo, and Jimeng Sun. 2016. Multi-layer representation learning for medical concepts.

- In *Proceedings of the 22nd ACM SIGKDD International Conference on Knowledge Discovery and Data Mining*. 1495–1504.
- [7] Edward Choi, Mohammad Taha Bahadori, Le Song, Walter F Stewart, and Jimeng Sun. 2017. GRAM: graph-based attention model for healthcare representation learning. In *Proceedings of the 23rd ACM SIGKDD international conference on knowledge discovery and data mining*. 787–795.
 - [8] Edward Choi, Cao Xiao, Walter F Stewart, and Jimeng Sun. 2018. Mime: Multilevel medical embedding of electronic health records for predictive healthcare. *arXiv preprint arXiv:1810.09593* (2018).
 - [9] Edward Choi, Zhen Xu, Yujia Li, Michael Dusenberry, Gerardo Flores, Emily Xue, and Andrew Dai. 2020. Learning the graphical structure of electronic health records with graph convolutional transformer. In *Proceedings of the AAAI Conference on Artificial Intelligence*, Vol. 34. 606–613.
 - [10] "Healthcare Cost and Utilization Project" (HCUP). 2016. HCUP clinical classifications software (CCS) for ICD-9-CM.
 - [11] Jacob Devlin, Ming-Wei Chang, Kenton Lee, and Kristina Toutanova. 2019. BERT: Pre-training of Deep Bidirectional Transformers for Language Understanding. In *Proceedings of the 2019 Conference of the North American Chapter of the Association for Computational Linguistics: Human Language Technologies, Volume 1 (Long and Short Papers)*. Association for Computational Linguistics, Minneapolis, Minnesota, 4171–4186. <https://doi.org/10.18653/v1/N19-1423>
 - [12] Yu Gu, Robert Tinn, Hao Cheng, Michael Lucas, Naoto Usuyama, Xiaodong Liu, Tristan Naumann, Jianfeng Gao, and Hoifung Poon. 2020. Domain-specific language model pretraining for biomedical natural language processing. *arXiv preprint arXiv:2007.15779* (2020).
 - [13] Varun Gulshan, Lily Peng, Marc Coram, Martin C Stumpe, Derek Wu, Arunachalam Narayanaswamy, Subhashini Venugopalan, Kasumi Widner, Tom Madams, Jorge Cuadros, et al. 2016. Development and validation of a deep learning algorithm for detection of diabetic retinopathy in retinal fundus photographs. *Jama* 316, 22 (2016), 2402–2410.
 - [14] Alistair EW Johnson, Tom J Pollard, Lu Shen, Li-wei H Lehman, Mengling Feng, Mohammad Ghassemi, Benjamin Moody, Peter Szolovits, Leo Anthony Celi, and Roger G Mark. 2016. MIMIC-III, a freely accessible critical care database. *Scientific data* 3 (2016), 160035.
 - [15] Zhenzhong Lan, Mingda Chen, Sebastian Goodman, Kevin Gimpel, Piyush Sharma, and Radu Soricut. 2019. Albert: A lite bert for self-supervised learning of language representations. *arXiv preprint arXiv:1909.11942* (2019).
 - [16] Isotta Landi, Benjamin S Glicksberg, Hao-Chih Lee, Sarah Cherng, Giulia Landi, Matteo Danieletto, Joel T Dudley, Cesare Furlanello, and Riccardo Miotto. 2020. Deep representation learning of electronic health records to unlock patient stratification at scale. *NPJ digital medicine* 3, 1 (2020), 1–11.
 - [17] Jinhyuk Lee, Wonjin Yoon, Sungdong Kim, Donghyeon Kim, Sunkyu Kim, Chan Ho So, and Jaewoo Kang. 2019. BioBERT: a pre-trained biomedical language representation model for biomedical text mining. *Bioinformatics* (09 2019). <https://doi.org/10.1093/bioinformatics/btz682>
 - [18] Yikuan Li, Shishir Rao, José Roberto Ayala Solares, Abdelaali Hassaine, Rema Ramakrishnan, Dexter Canoy, Yajie Zhu, Kazem Rahimi, and Gholamreza Salimi-Khorshidi. 2020. BEHRT: transformer for electronic health records. *Scientific reports* 10, 1 (2020), 1–12.
 - [19] Zachary C Lipton, David C Kale, Charles Elkan, and Randall Wetzell. 2015. Learning to diagnose with LSTM recurrent neural networks. *arXiv preprint arXiv:1511.03677* (2015).
 - [20] Yinhan Liu, Myle Ott, Naman Goyal, Jingfei Du, Mandar Joshi, Danqi Chen, Omer Levy, Mike Lewis, Luke Zettlemoyer, and Veselin Stoyanov. 2019. Roberta: A robustly optimized bert pretraining approach. *arXiv preprint arXiv:1907.11692* (2019).
 - [21] Fenglong Ma, Radha Chitta, Jing Zhou, Quanzeng You, Tong Sun, and Jing Gao. 2017. Dipole: Diagnosis prediction in healthcare via attention-based bidirectional recurrent neural networks. In *Proceedings of the 23rd ACM SIGKDD international conference on knowledge discovery and data mining*. 1903–1911.
 - [22] Fenglong Ma, Quanzeng You, Houping Xiao, Radha Chitta, Jing Zhou, and Jing Gao. 2018. Kame: Knowledge-based attention model for diagnosis prediction in healthcare. In *Proceedings of the 27th ACM International Conference on Information and Knowledge Management*. 743–752.
 - [23] Tomas Mikolov, Kai Chen, Greg Corrado, and Jeffrey Dean. 2013. Efficient estimation of word representations in vector space. *arXiv preprint arXiv:1301.3781* (2013).

- [24] Riccardo Miotto, Li Li, Brian A Kidd, and Joel T Dudley. 2016. Deep patient: an unsupervised representation to predict the future of patients from the electronic health records. *Scientific reports* 6, 1 (2016), 1–10.
- [25] Phuoc Nguyen, Truyen Tran, Nilmini Wickramasinghe, and Svetha Venkatesh. 2016. Deepr: a convolutional net for medical records. *IEEE journal of biomedical and health informatics* 21, 1 (2016), 22–30.
- [26] Yifan Peng, Shankai Yan, and Zhiyong Lu. 2019. Transfer Learning in Biomedical Natural Language Processing: An Evaluation of BERT and ELMo on Ten Benchmarking Datasets. In *Proceedings of the 2019 Workshop on Biomedical Natural Language Processing (BioNLP 2019)*. 58–65.
- [27] Jeffrey Pennington, Richard Socher, and Christopher D Manning. 2014. Glove: Global vectors for word representation. In *Proceedings of the 2014 conference on empirical methods in natural language processing (EMNLP)*. 1532–1543.
- [28] Trang Pham, Truyen Tran, Dinh Phung, and Svetha Venkatesh. 2016. Deepcare: A deep dynamic memory model for predictive medicine. In *Pacific-Asia conference on knowledge discovery and data mining*. Springer, 30–41.
- [29] Tom J Pollard, Alistair EW Johnson, Jesse D Raffa, Leo A Celi, Roger G Mark, and Omar Badawi. 2018. The eICU Collaborative Research Database, a freely available multi-center database for critical care research. *Scientific data* 5, 1 (2018), 1–13.
- [30] Alvin Rajkomar, Eyal Oren, Kai Chen, Andrew M Dai, Nissan Hajaj, Michaela Hardt, Peter J Liu, Xiaobing Liu, Jake Marcus, Mimi Sun, et al. 2018. Scalable and accurate deep learning with electronic health records. *NPJ Digital Medicine* 1, 1 (2018), 1–10.
- [31] Nina Rank, Boris Pfahringer, Jörg Kempfert, Christof Stamm, Titus Kühne, Felix Schoenrath, Volkmar Falk, Carsten Eickhoff, and Alexander Meyer. 2020. Deep-learning-based real-time prediction of acute kidney injury outperforms human predictive performance. *NPJ digital medicine* 3, 1 (2020), 1–12.
- [32] Laila Rasmy, Yang Xiang, Ziqian Xie, Cui Tao, and Degui Zhi. 2020. Med-BERT: pre-trained contextualized embeddings on large-scale structured electronic health records for disease prediction. *arXiv preprint arXiv:2005.12833* (2020).
- [33] Junyuan Shang, Tengfei Ma, Cao Xiao, and Jimeng Sun. 2019. Pre-training of graph augmented transformers for medication recommendation. *arXiv preprint arXiv:1906.00346* (2019).
- [34] Huan Song, Deepta Rajan, Jayaraman Thiagarajan, and Andreas Spanias. 2018. Attend and diagnose: Clinical time series analysis using attention models. In *Proceedings of the AAAI Conference on Artificial Intelligence*, Vol. 32.
- [35] Lihong Song, Chin Wang Cheong, Kejing Yin, William K Cheung, Benjamin CM Fung, and Jonathan Poon. 2019. Medical Concept Embedding with Multiple Ontological Representations.. In *IJCAI*. 4613–4619.
- [36] Ethan Steinberg, Ken Jung, Jason A. Fries, Conor K. Corbin, Stephen R. Pfohl, and Nigam H. Shah. 2021. Language models are an effective representation learning technique for electronic health record data. *Journal of Biomedical Informatics* 113 (2021), 103637. <https://doi.org/10.1016/j.jbi.2020.103637>
- [37] Ashish Vaswani, Noam Shazeer, Niki Parmar, Jakob Uszkoreit, Llion Jones, Aidan N Gomez, Lukasz Kaiser, and Illia Polosukhin. 2017. Attention is All you Need. In *Advances in Neural Information Processing Systems*, I. Guyon, U. V. Luxburg, S. Bengio, H. Wallach, R. Fergus, S. Vishwanathan, and R. Garnett (Eds.), Vol. 30. Curran Associates, Inc., 5998–6008. <https://proceedings.neurips.cc/paper/2017/file/3f5ee243547dee91fbd053c1c4a845aa-Paper.pdf>
- [38] Zhilin Yang, Zihang Dai, Yiming Yang, Jaime Carbonell, Ruslan Salakhutdinov, and Quoc V Le. 2019. Xlnet: Generalized autoregressive pretraining for language understanding. *arXiv preprint arXiv:1906.08237* (2019).
- [39] Changchang Yin, Rongjian Zhao, Buyue Qian, Xin Lv, and Ping Zhang. 2019. Domain Knowledge guided deep learning with electronic health records. In *2019 IEEE International Conference on Data Mining (ICDM)*. IEEE, 738–747.
- [40] Muhan Zhang, Christopher R King, Michael Avidan, and Yixin Chen. 2020. Hierarchical Attention Propagation for Healthcare Representation Learning. In *Proceedings of the 26th ACM SIGKDD International Conference on Knowledge Discovery & Data Mining*. 249–256.

- [41] Yukun Zhu, Ryan Kiros, Rich Zemel, Ruslan Salakhutdinov, Raquel Urtasun, Antonio Torralba, and Sanja Fidler. 2015. Aligning Books and Movies: Towards Story-Like Visual Explanations by Watching Movies and Reading Books. In *Proceedings of the 2015 IEEE International Conference on Computer Vision (ICCV) (ICCV '15)*. IEEE Computer Society, USA, 19–27. <https://doi.org/10.1109/ICCV.2015.11>

A AUPRC Results from Pre-Trained Text Encoders with Different Sizes and Pre-Training Techniques

Table 4: Results of BERT variation models on eICU

Task	Model	BERT-tiny	BERT-mini	BERT-small	BERT	Bio-BERT	Bio-clinical-BERT	Blue-BERT
Dx	CLS-FT	0.557	0.559	0.558	0.556	0.556	0.558	0.559
	FT-BERT	0.594	0.595	0.595	0.591	0.59	0.593	0.591
Mort	CLS-FT	0.238	0.242	0.233	0.228	0.231	0.228	0.228
	FT-BERT	0.224	0.223	0.22	0.219	0.219	0.215	0.216
LOS>3	CLS-FT	0.528	0.528	0.526	0.524	0.527	0.525	0.526
	FT-BERT	0.536	0.527	0.523	0.523	0.522	0.528	0.526
LOS>7	CLS-FT	0.229	0.233	0.228	0.222	0.223	0.226	0.228
	FT-BERT	0.22	0.218	0.215	0.214	0.213	0.217	0.215
ReAdm	CLS-FT	0.194	0.239	0.238	0.231	0.239	0.223	0.237
	FT-BERT	0.289	0.283	0.278	0.276	0.277	0.281	0.275

Table 5: Results of BERT variation models on MIMIC-III

Task	Model	BERT-tiny	BERT-mini	BERT-small	BERT	Bio-BERT	Bio-clinical-BERT	Blue-BERT
Dx	CLS-FT	0.752	0.754	0.755	0.757	0.755	0.755	0.754
	FT-BERT	0.771	0.77	0.77	0.767	0.769	0.769	0.767
Mort	CLS-FT	0.339	0.345	0.34	0.344	0.339	0.338	0.335
	FT-BERT	0.378	0.371	0.365	0.362	0.363	0.363	0.364
LOS>3	CLS-FT	0.616	0.614	0.615	0.615	0.611	0.61	0.608
	FT-BERT	0.624	0.623	0.623	0.621	0.626	0.622	0.62
LOS>7	CLS-FT	0.346	0.344	0.341	0.343	0.344	0.344	0.338
	FT-BERT	0.36	0.352	0.342	0.342	0.345	0.345	0.343
ReAdm	CLS-FT	0.044	0.043	0.044	0.045	0.044	0.045	0.044
	FT-BERT	0.043	0.043	0.044	0.043	0.045	0.043	0.043

Table 4 and Table 5 show AUPRC results differing in the size of pre-trained BERTs (BERT-tiny, BERT-mini, BERT-small, BERT) and in the domain-specific pre-training techniques (Bio-BERT, Bio-Clinical-BERT, Blue-BERT) in eICU and MIMIC-III respectively. In this experiment, we tested CLS-FT and FT-BERT for verifying the effectiveness of the variants. From the table, there is no consistent performance tendency among different sizes of BERTs and pre-training techniques across tasks and models with very marginal performance differences. Of note, large text encoders generally underperform smaller sizes of BERT. Contrary to our expectation, domain-specialized pre-training techniques rather harm the model performance compared to smaller sizes of BERTs. Overall, the size of the text encoder influences the performance greatly more than how pre-training techniques are modeled. For the experiments in the main paper, we choose BERT-tiny since it generally shows decent performance among other models and it requires less memory and computation time compared to the large models.

B PCA Results for Varied Random Seeds

We show the PCA results, while varying random seeds which result in a differently split dataset. Figure 6 shows the similar result with Figure 5 in the main paper.

C Detailed preprocessing method and table statistics

C.1 Detailed Preprocessing Information

In the following section we provide further detail about the construction of our datasets. As input for our predictive models, we employ three sources of information (we will further denote source of information as ‘item’ for simplicity)—laboratory, medication, and infusion—simultaneously for

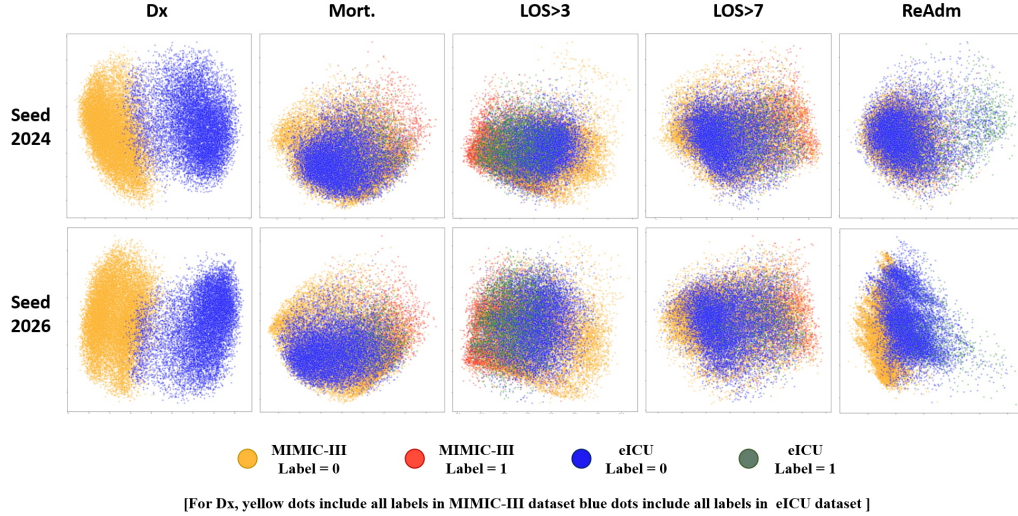


Figure 6: PCA visualizations on the ICU Representations for different random seeds.

each patient. The .csv files corresponding to each item are described in Table 6. Note that when merging MIMIC-III files 'INPUTEVENTS_MV' and 'INPUTEVENTS_CV', we remove 41 patient histories which straddle the transition between code systems and consequently are included partially in each file.

Table 6: File sources for each dataset

Item	Source	Filename
Lab	MIMIC-III	LABEVENTS.csv
Lab	eICU	lab.csv
Med	MIMIC-III	PRESCRIPTIONS.csv
Med	eICU	medication.csv
Inf	MIMIC-III	INPUTEVENTS.csv
Inf	eICU	infusionDrug.csv

For the sake of comparability, we built patients cohorts from the full MIMIC-III and eICU databases based on the following criteria: (1) Medical ICU (MICU) patients (2) over the age of 18 who (3) remain in the ICU for over 12 hours. We operationalize criterion (1) in MIMIC-III as patients for whom the first care unit is the last care unit and ICU type is MICU (i.e. we exclude patients who have transferred ICUs). For patients with multiple ICU stays, we draw exclusively on the first stay, and we remove any ICU stays with fewer than 5 observed codes. Within each ICU stay, we restrict our sample to the first 150 codes during the first 12 hours of data, and remove codes which occur fewer than 5 times in the entire dataset. Code sequence is determined by the associated time stamp.

C.2 Predictive Task Labels

We predict patient outcomes across five tasks: readmission, mortality, an ICU stay exceeding three or seven days, and diagnosis prediction. The first four are binary classification, the last multi-label. The variable-level criteria to generate these labels is available in Table 8.

In order to generate diagnosis labels for comparison across datasets, we employ the Clinical Classifications Software (CCS) for ICD-9-CM of the Healthcare Cost and Utilization Project [10]. We utilize the highest level representation available of ICD9 diagnosis, a common code format across EHR. There are 18 such representations. MIMIC-III and eICU diagnoses represented by ICD9 codes are simply mapped using the CCS classification. eICU ICD10 diagnoses are mapped first to ICD9

Table 7: Prediction dataset summary statistics

Statistic	eICU	MIMIC-III
<i>N</i> Observations	12,818	18,536
<i>N</i> ICU Stays	12,818	18,536
<i>N</i> Hospital Adm.	12,818	18,536
<i>N</i> Patients	12,818	18,536
Mean Seq. Length	48.8	65.3
Median Seq. Length	43.0	57.0
<i>N</i> Total Codes	625,594	1,211,107
<i>N</i> Unique Codes	2,018	2,855

codes before to their CCS classification. Finally, for eICU string diagnoses (e.g. Infection ... | ... bacterial ... | ... tuberculosis), we first search the most granular level for a string match with ICD9 before proceeding up the hierarchy for a match.

Table 8: Specific label criteria

Target	eICU	MIMIC-III
Readmission	Count('patientUnitStayID') >1	Count('ICUSTAY_ID') >1
Mortality	'unitDischargeStatus' == 'Expired'	'DOD_HOSP' not null
LOS >3 Days	'unitDischargeOffset' >3*24*60	LOS >3
LOS >7 Days	'unitDischargeOffset' >7*24*60	LOS >7
Diagnosis	set('diagnosisstring') per 1 ICU	ICD9_CODE-LONG_TITLE

C.3 Data Statistics

After preprocessing input data, we found that some patients lack all three items. Consequently, in some cases the item was left out from the patient dataset. For example, some patients have all the items in the code sequence, while others are included without all of them. In the MIMIC-III and eICU we use, the size of the entire dataset is the same as the union shown in Table 7 for each of the source dataset.

C.4 Hyperparameters

We conducted the hyperparameter searching experiment in CodeEmb and DescEmb on MIMIC-III and eICU. We swept the hyperparameter space within a fixed range, presented below, by grid search.

- dropout = [0.1, 0.3, 0.5]
- embedding dimension = [128, 256, 512, 768]
- hidden dimension = [128, 256, 512]
- learning rate = [5e-4, 1e-4, 5e-5, 1e-5]

We spent over 72 hours trying to find the best hyperparameter set for each case. We noticed that hyperparameters did not significantly affect the final result. For the experiment's simplicity, we unified one hyperparameter set for all cases without greatly harming each individual model's performance. The final set results are dropout of 0.3, embedding dimension and hidden dimension for the predictive model as 128 and 256 respectively, and learning rate of 1e-4.